



CHORUS

This is the accepted manuscript made available via CHORUS. The article has been published as:

Updated β -decay measurement of neutron-rich ^{74}Cu

J. L. Tracy, Jr. *et al.*

Phys. Rev. C **98**, 034309 — Published 10 September 2018

DOI: [10.1103/PhysRevC.98.034309](https://doi.org/10.1103/PhysRevC.98.034309)

An Updated β -Decay Measurement of Neutron-Rich ^{74}Cu

J. L. Tracy Jr,¹ J. A. Winger,¹ B. C. Rasco,² U. Silwal,¹ D. P. Siwakoti,¹ K. P. Rykaczewski,³
R. Grzywacz,^{2,3,4} J. C. Batchelder,⁵ C. R. Bingham,^{2,3} N. T. Brewer,⁶ L. Cartegni,⁴ A. A. Ciemny,⁷
A. Fijałkowska,^{2,7} C. J. Gross,³ C. Jost,² M. Karny,^{7,8} K. Kolos,² A. Korgul,⁷ W. Królas,⁹ Y. Liu,³
M. Madurga,² C. Mazzocchi,⁷ A. J. Mendez II,^{3,10} K. Miernik,^{3,7} D. Miller,² S. Padgett,²
S. V. Paulauskas,² D. W. Stracener,³ M. Wolińska-Cichočka,^{3,8,11} M. M. Rajabali,¹² and E. F. Zganjar¹³

¹*Dept. of Physics and Astronomy, Mississippi State University, Mississippi State, Mississippi 39762, USA*

²*Dept. of Physics and Astronomy, University of Tennessee, Knoxville, Tennessee 37996, USA*

³*Physics Division, Oak Ridge National Laboratory, Oak Ridge, Tennessee 37831, USA*

⁴*Joint Institute for Nuclear Physics and Applications, Oak Ridge, Tennessee 37996, USA*

⁵*Department of Nuclear Engineering, University of California, Berkeley, California 94702, USA*

⁶*Dept. of Physics and Astronomy, Vanderbilt University, Nashville, Tennessee 37235, USA*

⁷*Dept. of Physics, University of Warsaw, PL 02-093 Warsaw, Poland*

⁸*Oak Ridge Associated University, Oak Ridge, Tennessee 37831, USA*

⁹*Institute for Nuclear Physics, Polish Academy of Sciences, PL 31-342, Kraków, Poland*

¹⁰*Austin Peay State University, Clarksville, Tennessee, 37044, USA*

¹¹*Heavy Ion Laboratory, University of Warsaw, Warsaw PL 02-093, Poland*

¹²*Tennessee Tech University, Cookeville, Tennessee 38505, USA*

¹³*Department of Physics and Astronomy, Louisiana State University, Baton Rouge, Louisiana 70803, USA*

(Dated: August 19, 2018)

The β decay of neutron-rich ^{74}Cu has been studied at the Holifield Radioactive Ion Beam Facility at Oak Ridge National Laboratory. By using a high-resolution mass separator a purified ^{74}Cu beam was obtained, thus allowing decay through its isobar chain to stable ^{74}Ge without any decay chain member dominating. A total of 170 γ rays were associated with ^{74}Cu β decay with 111 placed in the ^{74}Zn level scheme. Updated β feeding intensities and estimated $\log(ft)$ values are presented, and new J^π assignments are proposed using shell model calculations. The progression of simulated Total Absorption γ -ray Spectroscopy (TAGS) based on proposed levels and β -feeding values from previous measurements to this evaluation are presented and demonstrate the need for a TAGS measurements for this and similar decays.

I. INTRODUCTION

The decay profile of radioactive fission products of heavy nuclei is of major importance to the development of next-generation nuclear power plants [1]. This profile, called *decay heat*, is essentially a map of the total energy emitted during these decays toward stability. Attempts to model the decay heat as a function of time have been made using available data for the fission daughters [1, 2]. Specific attention has been drawn to the period from 300 to 3000 s after the reactor has been shut down, a time during which the decay heat calculations may be improperly determined with current models [3]. For a given fissioning nuclide (e.g. ^{235}U), β and γ -ray emission together may carry on the order of 14 MeV of energy from the daughters. Due to efficiency and resolution limitations for Ge detectors used in high-resolution γ -ray spectroscopy, the γ -ray energy actually released by a decaying nuclide is not fully accounted for in the decay schemes measured in the laboratory, a discrepancy that is propagated into the decay heat calculations. This discrepancy between predicted decay heat and actual energy released is associated with the *pandemonium effect* in which a large Q_β window results in allowed β decay to an essentially continuous distribution of states above a few MeV of excitation energy resulting in a large number of extremely weak γ -ray transitions to lower-lying states

which fall below the detection limit of the equipment [4]. The failure to include feedings to higher-lying states results in overestimation of the β -decay energy and an incorrect β strength function. Nuclei for which this occurs are labeled as part of the *pandemonium problem* [3]. Algora *et al.* have suggested that when the highest known energy level directly fed in a β -decay daughter is less than 70% of the total Q_β window, values of E_β and E_γ should revert to theoretical values [5].

Work done by Yoshida *et al.* [9] and Algora *et al.* [5] has brought attention to the fact that the type of measurement from which level schemes are developed has a significant influence over understanding of the pandemonium problem. In their works, it is demonstrated that total absorption γ -ray spectroscopy (TAGS) leads to improvements in the decay heat calculations. This is due to the high efficiency of a TAGS detector array, which is able to sum the γ -ray energies emitted in cascades from high-lying states fed directly by β decay of the parent. This avoids the problem from high-resolution and low-efficiency detectors in which very weak transitions and/or high-energy transitions (often corresponding to decays from high-lying states) are more difficult to detect.

The β decay of ^{74}Cu has been studied previously using high-resolution techniques. The Q_β of ^{74}Cu is rather high at 9751(7) keV [6]. The first study, performed by Winger

et al. [7], found just 19 γ rays and placed them among ten excited states up to just under 3.0 MeV excitation energy. The second study by Van Roosbroeck *et al.* [8] yielded a much cleaner production of ^{74}Cu by using selective laser ionization. Their work was able to propose an improved level scheme of 21 levels using 32 placed γ rays, extending the scheme up to 5.6 MeV. However, despite having improved the known level scheme for ^{74}Cu , Van Roosbroeck *et al.*'s scheme only raised the expectation that there are a significant number of high-lying levels that must exist but had not been observed.

The work presented here will demonstrate a significant increase in our knowledge of the middle-range states (~ 3 -6 MeV) in ^{74}Zn fed by the β decay of ^{74}Cu measured using an HPGe detector array. Additionally, we will be able to present a list of γ rays belonging to ^{74}Cu decay that could not be placed in the level scheme because of insufficient statistics in the γ - γ coincidence spectra. These results will show the pandemonium effect becoming very apparent for this decay.

II. EXPERIMENT

The experiment was performed at the Holifield Radioactive Ion Beam Facility (HRIBF) at Oak Ridge National Laboratory (ORNL). A 54 MeV proton beam was generated by the Oak Ridge Isochronous Cyclotron (ORIC) and impinged upon a uranium carbide (UC_x) target, inducing fission. The fission daughters were thermalized and ionized in a hot plasma ion source, then extracted as a positively-charged ion beam which was directed through a mass separator with resolution $M/\delta M \sim 600$ for isobaric separation to $A = 74$. In the original experiment performed by Winger *et al.*, which used a similar beam production method, ^{74}Zn was also produced but implanted at a much higher rate than ^{74}Cu , limiting the results in the analysis. Specifically, the presence of γ rays from the ^{74}Zn β decay overwhelmed those from the ^{74}Cu β decay, making it difficult to distinguish all but the strongest transitions from any newly-measured weak ^{74}Zn γ rays sitting on a large statistical background. This issue was also a factor in the experiment performed by Van Roosbroeck *et al.*, despite the fact that they used a laser-ionization source to specifically ionize the ^{74}Cu atoms (^{74}Zn and ^{74}Ga were ionized via surface ionization in the hot cavity). To resolve the daughter-dominance issue in the current experiment, the isobarically-resolved $A = 74$ beam was sent through a high-resolution isobar separator ($M/\delta M \sim 10,000$) to partially isolate ^{74}Cu from ^{74}Zn and ^{74}Ga . The purified ^{74}Cu beam was then sent to the Low-Energy Radioactive Ion Beam Spectroscopy Station (LeRIBSS) [10].

At LeRIBSS, the ions were implanted onto a moving tape collector (MTC) positioned at the center of a detector array and observed as they decayed. The detector array had two main components. First, a pair of plastic scintillators attached to the outside of the beam line,

each with $\sim 50\%$ solid angle coverage, which were used to detect β -electrons. Second, a high-purity germanium (HPGe) detector array to measure γ rays. The standard LeRIBSS configuration utilized four HPGe clover detectors; however, one detector was found to be defective and needed to be removed from the analysis. The three clover detector array had a collective absolute photopeak efficiency of 3.5% at 1.33 MeV.

A fully digital data acquisition system was used to collect data in triggerless mode in order to avoid data loss. The scintillators were used to tag β -decay events, while the HPGe detectors measured γ ray energies. All events were time-tagged, allowing offline generation of γ ray singles spectra as well as $\gamma\gamma$ coincidence matrices, both with or without a β -gate applied. Addback spectra were also generated within each clover detector. The γ -ray singles spectrum without addback was used to determine the γ ray energies and intensities in order to avoid β detection and γ -ray efficiency issues. The $\gamma\gamma$ matrices with and without addback were used in the coincidence analysis.

The γ -ray efficiency of the three clover detectors in the configuration used for this experiment was measured using standard γ -ray sources of ^{57}Co , ^{109}Cd , ^{137}Cs , ^{210}Po , ^{241}Am , ^{139}Ce , ^{113}Sn , ^{88}Y , and ^{60}Co for an energy range from 32 keV to 1836 keV. These results were compared with the efficiency values determined in previous experiments [10, 11] which used calibrated sources of ^{133}Ba , $^{152,154,155}\text{Eu}$, ^{137}Cs , ^{60}Co and ^{226}Ra for an energy range from 53 keV to 2204 keV, where the one defective detector in the current experiment was removed from the analysis of the previous calibration data. The results from the two efficiency measurements were in agreement, so a combined data set was used. In establishing the absolute photopeak efficiency, an estimated total γ -ray efficiency was determined based on a few data points to establish the ratio of total γ -ray efficiency to absolute photopeak efficiency thereby allowing summing corrections to be performed. The summing corrections brought the data points onto a smooth line, giving confidence in the total γ -ray efficiency curve even though it was not directly measured. Over the range from 300 keV to 3 MeV a log-log plot of absolute photopeak efficiency as a function of energy shows a linear behaviour. In order to extend the efficiency curve to energies above 3 MeV, we did a comparison of the behaviour of our detectors to other similar systems available in the literature [12–14]. Although the behaviour below 300 keV differs greatly, they all show a downward bend in the absolute photopeak efficiency starting at ~ 3.5 MeV. By adjusting the overall normalization and slightly adjusting the slope in the 300 keV to 2.2 MeV region, we obtained consistent values for the absolute photopeak efficiency in the 3 MeV to 9 MeV range allowing us to extrapolate the efficiency curve up to the 5 MeV range of our observed γ rays. The resulting data points were then fit to a six-term polynomial of $\log(\epsilon)$ versus $\log(E_\gamma)$ to obtain the efficiency curve. Both variance and covariance terms in the error matrix along

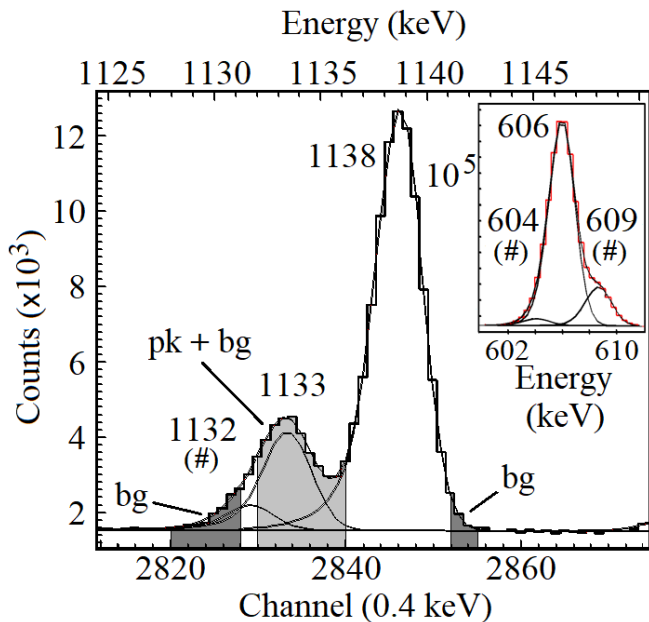


FIG. 1. Example of selective background gates used to isolate the coincidence spectrum of the 1133-keV transition. The peak gate is labeled by “pk + bg” and the background gates are labeled with “bg”. Peaks are labeled with γ -ray energy in keV; peaks belonging to the nuclide ^{74}Ga are labeled with (#). Inset is the compound 606-keV peak, to which this technique was applied to obtain the reasonably clean coincidence spectrum shown in Figure 3.

with χ^2_ν were used to determine the uncertainty in the fit efficiencies. The relative photopeak efficiencies, needed for determining the relative intensities, are known to less than 1% uncertainty for the range from 200 keV to 3 MeV and go up to several percent uncertainty on either end of the fitting range. The absolute photopeak and total γ -ray efficiencies used in the summing corrections have higher uncertainties, but these are a small effect on the uncertainty in the correction factor.

Within the $A = 74$ decay chain the half-lives are: $^{74}\text{Cu} - 1.63(5) s$, $^{74}\text{Zn} - 95.6(12) s$, and $^{74}\text{Ga} - 487(7) s$. The large differences in the half-lives makes it easy to enhance various members of the decay chain based on the MTC cycle used. The standard MTC cycle involves a grow in period when the activity was being collected on the tape while data were collected, a decay period in which the beam was deflected and the activity was allowed to decay while data were collected, and a move period during which the collected activity was moved to a shielded location while no data were collected. However, in this case it was determined that there was no need to run the MTC since no member of the decay chain dominated the γ -ray spectra. Four data runs were performed in the course of the experiment. Slight variations in the beam along with building of saturation provided different relative abundances of the members of the decay chain which assisted in the assignment of the γ rays. The first run which lasted 309 s was used to confirm the $A = 74$ mass

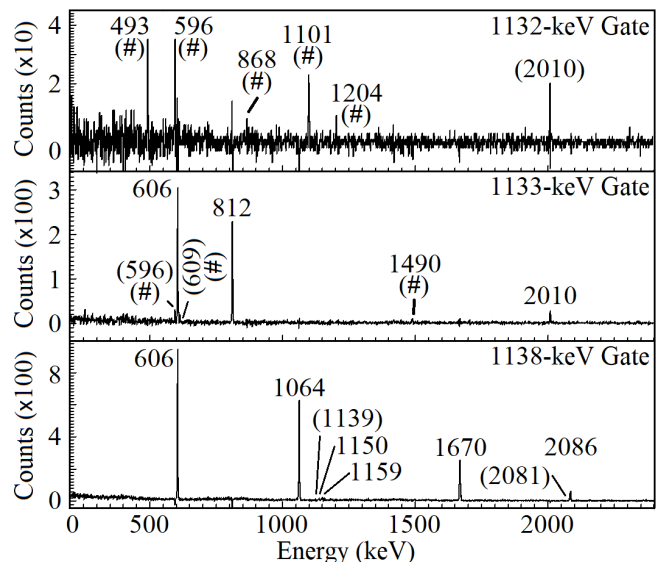


FIG. 2. Coincidence spectra of the three peaks seen in Figure 1 using the split-background technique described in the text. Numbers above the peaks give the coincident γ ray energy, with parenthesis indicating only a possible coincidence. All definite peaks in the 1132-keV gate (top panel) belong to the decay of ^{74}Ga , while all definite peaks in the other two gates are distinct, clean, and are only ^{74}Cu γ rays.

chain and that excessive amounts of ^{74}Zn and ^{74}Ga were not in the beam. The MTC was then moved to remove some observed residual contamination from a previous measurement. The last three runs did not involve moving the MTC, so they built the same saturation spot on the tape. The second and third runs, which lasted 3133 s and 2863 s, respectively, showed similar heights for the 606-keV γ ray from the ^{74}Cu decay and the 596-keV γ ray from the ^{74}Ga decay. The final run of 1810 s showed a 50% increase in the height of 596-keV γ ray to the 606-keV γ ray indicating a slight drift in the beam tune.

Raw spectra from each HPGe crystal were gain matched and energy calibrated using known γ rays from ^{74}Ga β decay along with low-energy transitions from ^{74}Zn and some higher energy ($> 3\text{ MeV}$) γ rays from ^{74}Cu where the energies were established using escape peaks. All spectra were then combined to generate both ungated and β -gated γ -ray singles spectra as well as $\gamma\gamma$ coincidence arrays at 0.4 keV per bin. The ungated γ -ray singles spectrum was analyzed to obtain γ -ray energies and relative intensities for all observable γ rays. In fitting the spectrum, global fit parameters were determined using well defined peaks and then held fixed during the fitting process.

Each γ ray in the list was then associated with one of the three decays in this mass chain based on time behavior in the MTC cycles, the effect of β -detection efficiency on each γ ray, and $\gamma\gamma$ coincidence information as will be discussed below. The LeRIBSS system has a β -detection efficiency which depends on the effective Q value for the

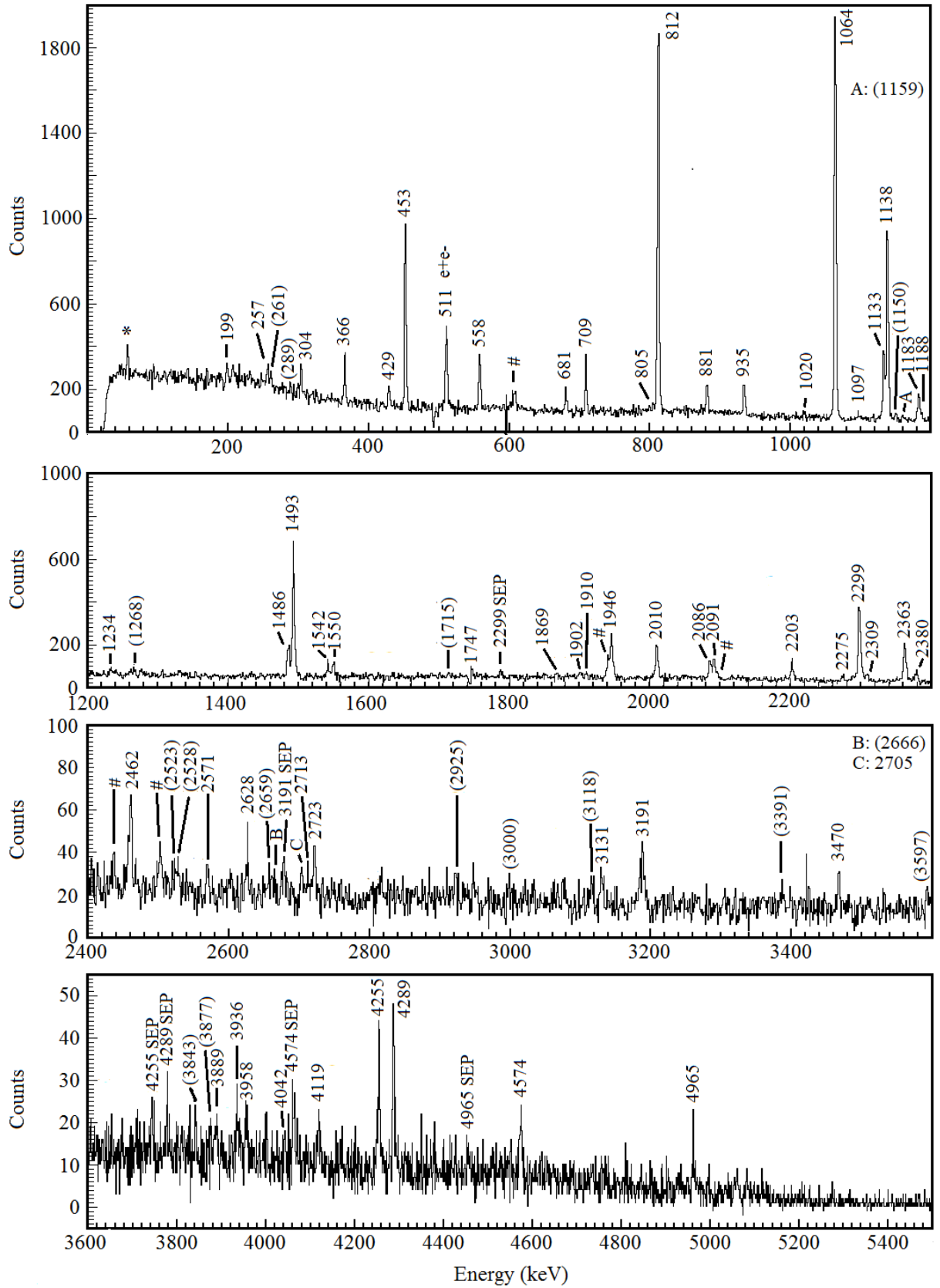


FIG. 3. The γ - γ -coincidence spectrum for the 606-keV peak. Probable coincidences are indicated in parentheses, and γ rays associated with ^{74}Zn (*) and ^{74}Ga (#) are indicated.

decay (see Ref. [15]). All γ rays associated with ^{74}Cu have a β -detection efficiency greater than 40%, while the other two decays have efficiencies less than 30%. This made it easy to identify proper assignment even for very weak peaks. Intensities for the ^{74}Cu γ rays were determined relative to the strongest transition at 606 keV. The final step in establishing the relative intensities was to perform a summing correction which first required establishing the decay scheme. Once the summing correction was applied, the intensities were recalculated and reported as the relative I_γ value for the respective γ ray.

The primary method for determining placement of a γ rays within a particular decay scheme was based on the coincidence information. The coincidence gating process was complicated by the frequent overlap of γ ray peaks. In many cases this made it impossible to use a single background gate to remove contamination from adjacent γ rays. This was even true for the primary ^{74}Cu γ ray at 606 keV which overlaps with the 604- and 609-keV γ rays from ^{74}Ga (Figure 1 inset). As an example, consider the gating method used for the 1133-keV γ ray shown in Figure 1. This γ -ray overlaps with an 1132-keV γ -ray from ^{74}Ga and an 1138-keV γ ray from ^{74}Cu . The large overlap on the low side of the peak forces low-side positioning of the peak plus background gate to be truncated to the right. Setting of the lower background gate was determined by the position which resulted in statistically equivalent peak areas in the gated spectra for γ rays associated with ^{74}Ga (the exception was the 596-keV γ ray which, along with the 606-keV γ ray, is in strong coincidence with all portions of the spectrum and could not be fully eliminated here). For the upper background gate, a clean gate on the 1138-keV peak was used to identify γ -ray coincidences and these were used to determine placement of the gate. A similar procedure was used for coincidence gating on all overlapping γ rays throughout the spectrum. For this particular grouping, the coincidence spectra for all three peaks are shown in Figure 2. Each panel shows reasonably clean and distinct spectra coincident with that given gate, specifically ^{74}Cu γ rays are observed as definite coincidences in the 1133- and 1138-keV gates while the definite coincidences in the 1132-keV gate are from ^{74}Ga . The background-subtracted coincidence spectrum for the principal 606-keV γ ray is shown in Figure 3, using the same technique to eliminate contributions from the 604- and 609-keV peaks. Some contaminant peaks are indicated, but were found to be statistically insignificant as discussed below.

Although the coincidence gating method used strived to provide clear evidence for the coincident γ rays, it is evident in Figure 3 that a simple qualitative visual inspection can lead to incorrect assumptions about actual coincidence relationships. To avoid this issue, we established a more quantitative method to determine definite or possible coincidence relationships. We fit the peak area in both the peak-plus-background gated spectrum

(A_P) and the background gated spectrum (A_B), determined the difference in the areas ($\Delta A = A_P - A_B$) as well as the uncertainty ($\sigma_{\Delta A}$), and defined a significance factor $S = \Delta A / \sigma_{\Delta A}$ for each observed γ ray in the spectrum. Hence, S is a measure of the statistical significance of an observed peak. If $S > 3.75$ then the coincidence was deemed to be definite (D), while $2.00 \leq S \leq 3.75$ indicated a possible coincidence (P). This method provided better confidence in the results, but can still lead to missing or extraneous information. For example, a weak γ -ray on a large background may in reality be in coincidence with the 606-keV γ ray, but does not show a statistical significance because the 606-keV γ ray is strong in both gate spectra. The selection of 3.75σ allows a $>99\%$ confidence level without eliminating valid but weak coincidences.

The purified nature of the beam yielded some advantages in fitting and gating of peaks which overlap nearby γ -ray peaks. The simple magnitude of the counts in a given peak in this data set ($\sim 13\times$ more than Van Roosbroeck *et al.* [8]) gave us more versatility in selecting both peak-plus-background and background gates, particularly for peaks which are part of blended multi-peaks. For example, the 1132-1133-1138-keV multi-peak shown in Figure 1 is one of the examples of troublesome compound peaks cited by Van Roosbroeck *et al.* The coincidence spectrum gated on the 1133-keV peak in their work included nine γ rays belonging to ^{74}Ga . In this work the coincidence spectrum (Figure 2, second panel) includes only the 609-keV (P) and the 1490-keV (D) peaks from ^{74}Ga . Our observed 1490-keV peak has a β -detection efficiency indicating only a ^{74}Ga component. The decay of ^{74}Ga has a reported peak at 1134 keV which, based on this coincidence information along with a gate on the 1490-keV γ ray, feeds the 1490-609-595 cascade. This is in agreement with the proposed assignment of an 1135-keV γ ray to ^{74}Ga decay by Van Roosbroeck *et al.*. Although directly fitting this peak is impossible, its $\sim 6\%$ contribution to the peak could be determined, and revised position and peak area information for the 1133-keV peak could be determined. The 1138-keV gate shows coincidence with an 1159.0 keV γ ray. The decay of ^{74}Ga has a known γ ray at 1160.3 keV which will be in coincidence with the 1940-keV γ ray [16]. Our 1940-keV gate shows a definite coincidence at 1160.4 keV. Furthermore, the relative intensity of the γ ray observed in the first fit of our data is larger (0.84(3)) than the NNDC value (0.69(5)). There is also no other evidence for an 1138-keV γ ray associated with ^{74}Ga . Hence, we propose an unresolved 1159.2(3) keV γ ray associated with ^{74}Cu decay where the intensity of the transition was determined from the coincidence data and a constrained fit of the singles spectrum, with the position determined from the constrained fit. Such unresolved doublets are frequently observed in the data.

TABLE I: Placed γ rays for ^{74}Cu β decay, along with the proposed energy level each de-excites, relative intensity, and $\gamma\gamma$ coincidence information. Probable coincidences are indicated with parentheses while those in italics are inconsistent with the proposed placement indicating a possible weaker unresolved component. See text for discussion.

γ -ray Energy (keV)	Level Energy (keV)	γ -ray Intensity (rel)	$\gamma\gamma$ Coincidences (keV)
158.74(19)	3063	0.113(21)	
198.67(7)	2551	0.44(3)	(812), 935, 1747
257.06(7)	2808	0.47(3)	(453), (606), (1133), (1946)
260.55(13)	3165	0.23(3)	(606), 1234, (1486), (2299)
288.64(6)	2986	0.49(3)	2091, (<i>2309</i>), 2697
304.05(5)	2657	0.74(3)	606, 812, 935, 2500
366.098(18)	3063	2.97(3)	606, 2091, (<i>2380</i>), 2508, 2565, 2646, 2697
428.82(4)	2099	0.95(4)	453, (558), (606), (709), 1064, 1670, (2523)
452.565(15)	2551	4.91(5)	257, 429, 606, 681, 812, 1493, (1670), (<i>1902</i>), 2010, (2309), (<i>2363</i>), (2523)
478.55(22)	2148	0.20(3)	1064
558.317(24)	2657	2.00(4)	(429), 606, 681, 1493, (1702), 2131, 2232, 2500
605.764(11)	606	100.0(10)	199, 257, (261), (289), 304, 366, 429, 453, 558, 681, 709, (805), 812, 881, 935, 1064, 1133, 1138, (1150), (1159), 1183, 1188, 1234, (1286), 1486, 1493, 1542, 1550, (1715), 1747, 1869, 1902, 1910, 1946, 2010, 2086, 2091, 2203, 2275, 2299, 2309, 2363, 2380, 2462, (2523), (2528), 2571, 2628, (2659), (2666), 2705, 2723, (2925), (3000), (3118), 3131, 3191, (3391), 3470, (3597), (3843), (3877), 3889, 3936, 3958, 4119, 4255, 4289, 4574, 4965
680.59(5)	2099	1.08(4)	453, (558), 606, 709, 812
709.398(22)	2808	2.30(3)	429, 606, 681, 1493, 2086
805.38(11)	2904	0.42(4)	(260), (606), 812, 1493
812.419(14)	1418	17.12(8)	199, 304, 453, 606, 681, 709, 935, 1097, 1133, 1238, (1446), 1486, 1550, 1715, 2010, 2028, 2309, 2500, 2571, 2666, 2805, (4542)
881.48(3)	2551	2.02(4)	257, 606, 1064, 1670, 2010, 2309, 2628
934.65(4)	2353	1.74(4)	199, 304, 606, 812, 2805
1020.13(12)	3572	0.39(3)	(812), (1747)
1064.212(17)	1670	20.63(9)	429, 606, 882, 1138, 1151, 1234, (1617), 1884, 1902, 2010, 2086, (2819), (3000), (3118), 3191, (3403), (3843)
1097.41(15)	2516	0.35(4)	812
1133.25(4)	2551	4.10(13)	(257), 606, 812, 2010, 2628
1138.458(18)	2808	17.52(7)	606, 1064, 1151, 1159, 1670, (2081), 2086, (2705), (2819)
1150.40(12)	3959	0.44(4)	(257), (606), (709), (1064), 1138, 1670
1159.2(3)	3968	0.39(7)	1138
1182.64(12)	1789	1.54(19)	606, 3105, (3935)
1187.61(22)	3287	0.30(4)	(606), 1064, 1493
1234.36(8)	2904	0.72(4)	606, 1064, 1670
1238.43(10)	2657	0.55(3)	812
1264.6(4)	2935	0.16(4)	(606), (1064), 1670
1267.66(24)	4076	0.32(5)	(1064), (1138)
1461.6(4)	3132	0.19(4)	(1064), 1670
1485.95(5)	2904	2.35(6)	606, 812, 2723
1493.15(3)	2099	10.27(8)	453, 558, 606, 709, 805, (1187), (1472), 2010, 2086, 2131, 3080
1542.40(7)	2148	0.91(4)	606, (2713), (3479)
1550.39(5)	2969	1.57(4)	(<i>453</i>), 606, 812, <i>1133</i> , <i>1138</i>
1617.13(21)	3287	0.29(4)	(<i>558</i>), 1064
1622.6(4)	4788	0.17(4)	
1669.95(3)	1670	10.20(6)	429, 882, 1138, (1151), 1234, (1265), 1902, 2010, 2086, (2371), (2406), (3000), (3118), 3191, (3219), (3843), 3957
1701.9(4)	4359	0.20(4)	(366), (606)
1715.23(18)	3133	0.39(4)	812
1747.26(22)	2353	0.82(18)	606
1868.7(4)	4420	0.25(5)	(453), 606, (1133)
1884.2(4)	3554	0.19(5)	(1064), (1670)
1901.59(8)	3572	1.18(5)	606, 1064, 1670
1909.92(19)	2516	0.36(4)	(606)
1945.82(5)	2551	3.39(9)	(257), 606, 2010, (2309), 2628
2010.12(5)	4562	4.71(7)	(247), 453, 606, 812, 882, (1064), 1133, 1493, 1670, 1946
2027.8(5)	3446	0.19(5)	812

γ -ray Energy (keV)	Level Energy (keV)	γ -ray Intensity (rel)	$\gamma\gamma$ Coincidences (keV)
2055.5(5)	5627	0.19(6)	(1064)
2081.4(7)	4890	0.16(7)	1138, 1493, 1670
2085.96(6)	4894	3.08(8)	606, 709, 1064, 1138, 1493, 1670, 2203
2091.30(6)	2697	2.02(7)	(289), 366, 606, (2164), (2646)
2130.77(15)	4788	0.70(6)	558, (1101), (1493)
2148.40(5)	2148	3.10(6)	2713, (3479)
2164.00(21)	4861	0.44(5)	2091, 2697
2202.81(6)	2808	1.78(5)	606, 2086
2211.04(19)	5180	0.46(5)	2363
2232.85(19)	4890	0.62(5)	(304), (558), 1493
2275.3(3)	5180	0.32(6)	606, 2298
2298.67(5)	2904	7.71(7)	(260), 606, 2666, 2723
2309.22(10)	4861	0.93(4)	(289), 453, 606, 812, 882, 1133, 1946
2363.01(6)	2969	4.65(5)	453, 606, 2188, 2211, 2659
2371.3(3)	5180	0.25(4)	(606), (1138), (1670)
2379.63(8)	2986	1.12(4)	366, 606
2406.3(4)	4076	0.18(4)	(1064), 1670
2461.50(15)	3067	1.04(8)	606, (2508)
2500.3(3)	5158	0.43(6)	558, 606, (681), (812), 1493
2507.46(19)	5570	0.60(5)	366, (606), 1064
2522.6(7)	5074	0.12(4)	(429), 453
2527.6(3)	5513	0.27(4)	(606), (2380)
2564.6(3)	5627	0.22(4)	366
2570.72(24)	3989	0.28(3)	606, 812, 1493, (1946)
2627.82(13)	5180	0.66(4)	(882), (1493), 1946
2645.9(4)	5709	0.19(4)	366, 2091, 2697
2659.27(23)	5627	0.36(4)	2363
2665.6(3)	5570	0.26(4)	(606), (1064), (1493), 2299
2697.00(10)	2697	2.44(9)	289, 366, (2164), 2565, (2646)
2704.9(3)	5513	0.33(4)	(606), 1138
2712.72(15)	4861	0.54(4)	(606), 1542, 2148
2722.81(11)	5627	1.13(5)	606, (812), (1486), 2299
2741.6(7)	4890	0.12(4)	
2804.8(4)	5158	0.19(4)	(812), (935)
2818.53(19)	5627	0.48(4)	(1064), 1138, (1670)
2924.6(3)	3530	0.24(3)	606
2999.78(20)	4670	0.46(4)	(606), 1064, (1670)
3018.8(4)	5570	0.20(4)	
3080.9(6)	5180	0.28(7)	1493
3104.8(4)	4894	0.22(10)	1183
3118.0(3)	4788	0.34(3)	606, (1064), 1670
3131.36(22)	3737	0.50(4)	606
3190.57(14)	4861	1.31(4)	606, 1064, 1670
3364.8(3)	5513	0.30(4)	(2148)
3390.6(6)	5180	0.17(4)	606, (812)
3403.4(5)	5074	0.21(4)	1064
3470.41(25)	4076	0.46(4)	606
3479.4(5)	5627	0.18(3)	1542, 2148
3487.6(5)	5158	0.18(3)	(606), 1064, (1670)
3610.1(6)	5709	0.21(5)	
3842.9(5)	5513	0.26(4)	606, 1064, (1493) (1670)
3888.9(4)	4495	0.35(4)	606, (1138)
3935.5(4)	5724	0.39(4)	606, 935, 1183, (1670)
3957.56(24)	5627	0.95(4)	(606), 1064, 1670
4041.6(8)	4647	0.17(11)	606
4119.0(4)	4725	0.36(4)	606
4255.4(3)	4861	1.48(5)	606, (1064)
4288.7(3)	4894	1.67(5)	606
4574.3(3)	5180	0.95(5)	606
4907.4(6)	5513	0.12(3)	(606)

γ -ray Energy (keV)	Level Energy (keV)	γ -ray Intensity (rel)	$\gamma\gamma$ Coincidences (keV)
4965.6(4)	5570	0.53(4)	606
5020.8(5)	5627	0.124(22)	(606)

III. DECAY SCHEME OF ^{74}Cu

With the coincidence relationships established, it was possible to develop the ^{74}Zn level scheme. At total of 170 γ rays were associated with ^{74}Cu β decay. Of these, 111 were placed in the ^{74}Zn level scheme, which consists of 50 levels. The specific details for each γ ray placed into the scheme are listed in Table I, with the proposed decay scheme shown in Figure 4 and Figure 5, while the 59 unplaced γ rays are listed in Table II. A summary of the proposed level energies, β feedings, and $\log(ft)$ value lower limits are presented in Table III. Levels presented are based on several criteria. First, levels with two or more decays out established by coincidence relationships, a single decay out with a statistically definite coincidence observed both ways, or an observed statistically significant cascade seen from above are shown with solid horizontal lines indicating strong confidence in the existence of the level. Second, those without solid evidence but which are consistent with the coincidence data are presented as dashed lines indicating possible existence of a level. In Table I, some cases occur where a γ ray shows a coincidence inconsistent with the proposed placements suggesting a weak unresolved doublet. These inconsistent coincidence are indicated by italicized text in the table. For such cases, all the intensity listed has been assigned to the stronger component. The unplaced γ rays represent 4.4% of the total identified ^{74}Cu γ -ray intensity, while the unassigned intensity is less than 1%. The inability to place these γ rays was due to either inconsistent coincidence data making a definite placement difficult or a total lack of any coincidence data. Furthermore, energy sums and differences do not provide firm evidence for establishment of any additional new levels. Handling of the unplaced transitions will be discussed in more detail later.

Overall, the new level scheme expands that proposed by Van Roosbroeck *et al.* by adding 29 new excitation levels up to 5724 keV, more than doubling the number of levels in the previous scheme. The placement of 79 new γ rays into this scheme, by lowering the relative intensity limit from $\sim 1\%$ to $\sim 0.2\%$, more than triples our overall knowledge of the decay behavior over what was previously known.

A. Below 3.1 MeV

All of the level scheme proposed by Van Roosbroeck *et al.* [8] is preserved below 3.1 MeV (see Figure 4). However, 14 previously unknown transitions have been added in this region along with one definite and one tentative

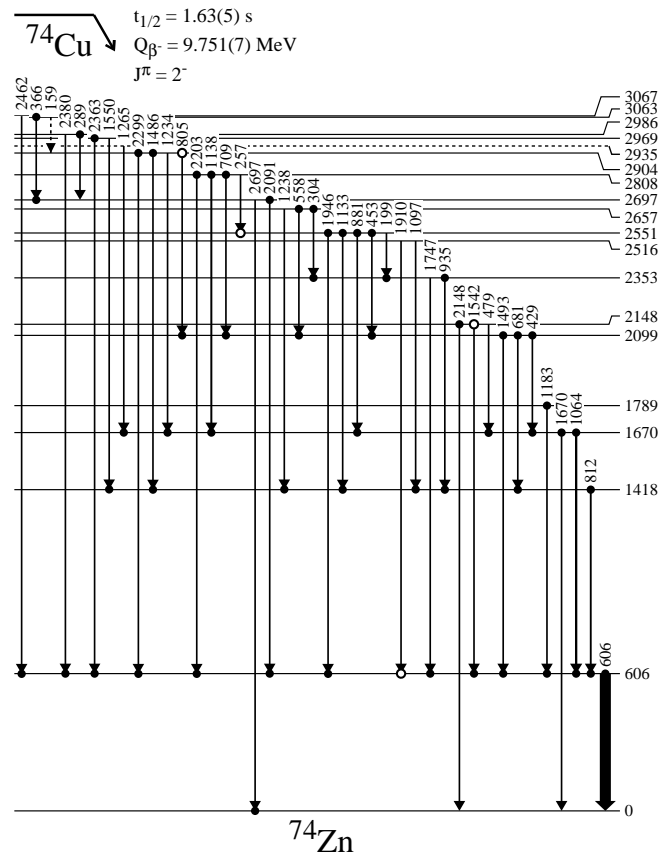


FIG. 4. Proposed decay scheme for ^{74}Cu determined in this analysis in the energy region below 3.1 MeV. See Section III-A for discussion. Solid dots indicate definite coincidences, while open dots indicate possible coincidences based on the statistical tests mentioned in the text.

new level. In the Van Roosbroeck *et al.* experiment, the production of ^{74}Cu was enhanced by using a laser-ionization ion source. Their method did not prevent the production of other $A = 74$ isotopes, so in order to generate a relatively clean spectrum from implanted ^{74}Cu decays, β -gated spectra of equivalent collection times were made with the laser enhancement on and then off. The laser-off spectrum was normalized to the laser-on spectrum using the ratio of peak height counts for the 868-keV γ ray from ^{74}Ga . The normalized laser-off spectrum was then subtracted from the laser-on spectrum. While this technique effectively removed most contaminant peaks originating from implanted ^{74}Ga , some peaks were found to be over-subtracted, leading to gaps in the subtracted spectrum. Furthermore, by scaling the laser-

TABLE II. Unplaced γ rays associated with ^{74}Cu β decay. See text for details.

γ -ray Energy (keV)	γ -ray Intensity (rel)	$\gamma\gamma$ Coincidences (keV)	γ -ray Energy (keV)	γ -ray Intensity (rel)	$\gamma\gamma$ Coincidences (keV)	γ -ray Energy (keV)	Intensity Intensity (rel)	$\gamma\gamma$ Coincidences (keV)
247.5(5)	0.053(23)		3056.3(4)	0.21(4)		4624.5(7)	0.21(4)	
423.9(3)	0.14(4)		3065.3(4)	0.34(4)		4671.8(12)	0.28(6)	812
516.12(16)	0.35(4)		3070.2(10)	0.12(4)		4698.5(16)	0.20(5)	
1007.7(4)	0.10(3)		3218.5(4)	0.20(3)	(1064), (1670)	4738.1(7)	0.12(3)	(606)
1038.4(3)	0.13(3)		3597.1(3)	0.39(4)	(606)	4790.2(5)	0.20(3)	606
1067.16(18)	0.42(5)	(812)	3726.6(11)	0.10(4)		4810.2(8)	0.11(3)	(606)
1306.4(5)	0.10(3)	(606), (2298)	3793.9(4)	0.34(4)		4831.5(4)	0.39(3)	
1378.0(3)	0.20(3)	(606)	3877.0(5)	0.22(4)		4892.6(8)	0.10(3)	606
1446.65(18)	0.45(5)	(812)	3902.1(7)	0.16(4)		4946.4(8)	0.14(4)	
1581.0(3)	0.20(4)	(366)	4002.3(6)	0.18(4)	606	4999.4(6)	0.14(3)	(606)
1720.6(5)	0.13(4)	(289)	4144.5(7)	0.17(4)		5040.3(5)	0.25(3)	
2177.70(21)	0.44(5)	(366), (1064)	4156.8(4)	0.39(4)	(606)	5054.7(6)	0.14(3)	
2413.5(6)	0.12(3)	(366)	4171.6(6)	0.21(4)	606	5086.9(8)	0.22(4)	
2424.2(4)	0.18(3)		4202.3(12)	0.10(4)		5105.0(13)	0.11(3)	
2448.51(22)	0.33(3)	(1064), (1138)	4432.9(5)	0.33(4)	606	5125.5(8)	0.20(3)	606
2617.9(4)	0.22(4)	(1138)	4497.6(10)	0.15(4)		5184.9(15)	0.065(18)	
2642.5(6)	0.12(4)	(2697)	4542.5(3)	0.82(5)		5233.8(14)	0.047(12)	
2762.0(5)	0.16(4)	(1064)	4581.6(9)	0.19(4)		5439.3(13)	0.13(5)	
2912.5(3)	0.24(3)	(1064)	4592.2(8)	0.18(4)		5487.1(7)	0.19(6)	
3043.0(4)	0.19(3)		4615.9(7)	0.23(4)				

off spectrum to match the laser-on spectrum, background variations were also magnified. The subtraction of the two spectra therefore transferred those magnified statistics to the laser-on data, ultimately obscuring weaker peaks. Most prominently, this contributed to an incorrectly reduced I_β value for the 1418-keV level, as will be discussed later. Although they were able to extend the Winger *et al.*[7] scheme and remove a couple of wrongly placed γ rays, the Van Roosbroeck *et al.* data still suffered from the loss of weaker peaks. In the current work, the new transitions placed below 3.1 MeV are all comparatively weak, with none exceeding a relative intensity of $\sim 1.8\%$. The new 2516-keV level is established by mutual coincidences (812-1097 and 606-1910), while the tentative level at 2935 keV is supported by a mutual coincidences but lacks statistical significance in both directions.

Of the newly-placed transitions, the 2203-keV transition was lost in the Van Roosbroeck *et al.* subtraction approach. In Figure 1 of their paper, a double peak around 2200 keV can be seen in the laser-on spectrum, a single larger peak at this energy in the laser-off spectrum, and an over-subtracted gap in the subtracted spectrum. The placement of the 2203-keV γ ray in our proposed scheme shows a transition directly to the 606-keV 2^+ state, thus limiting the spin and parity assignments for the 2808-keV energy level.

In our data, a weak 1265-keV peak overlaps with an equally-weak 1268-keV peak. As shown in Table I, both of these γ rays indicate coincidence with ^{74}Cu lines. To further complicate the matter, in the coincidence spectrum of the 1670-keV γ ray is a very weak peak around 1266 keV. Indeed, this coincidence peak has only 14

counts in its fit of the peak area, and the Gaussian fit of this coincident peak showed a centroid at 1266.2 keV. The significance factor for this peak was 2.45, making this coincidence probable/possible. The coincidence spectrum of the 1265-keV γ ray showed the 1670-keV γ ray in coincidence, while the 1268-keV γ ray did not. Based on these factors, it was decided to place the 1265-keV γ ray into the decay scheme de-exciting the possible new level at 2935 keV, while the possible coincidence between the 1268-keV γ ray and the 1138-keV γ ray supports placement feeding the 2808-keV level.

In the scheme by Winger *et al.*, two levels at 1164 keV and 2616 keV were placed that were later removed by Van Roosbroeck *et al.*. The first level was based on the 558-keV γ ray showing only a coincidence with 606-keV γ ray. Van Roosbroeck *et al.* also observe coincidence with the 1493-keV γ ray and proposed the transition to de-excite a new level at 2657 keV. In our data, the 558-keV γ ray is also observed to be coincident with the 606- and 1493-keV γ rays, but now the 429-keV γ ray is shown to be a probable coincidence, thus confirming placement of the 558-keV γ ray. The 2616-keV level proposed by Winger *et al.* was based on coincidence between the 606- and 2010-keV γ rays with a 517-keV crossover transition to the 2099-keV level. Our data, along with that of Van Roosbroeck *et al.*, shows a large number of γ rays in coincidence the 2010-keV γ ray supporting its placement as de-exciting a level at 4562 keV. Existence of the 517-keV γ ray is then called into question. Winger *et al.* observed weak peaks at 505 and 517 keV, either side of the broad 511-keV annihilation peak. The fit of our data indicates the 505-keV peak to be much weaker than the 517-keV

peak in contradiction to Winger *et al.*. Furthermore, the β efficiency suggests the 505-keV peak comes from ^{74}Zn β decay. The 511-keV peak does exhibit a structure on the high energy side indicating a γ ray. A good fit of the data requires two γ -rays (514.2 and 516.1 keV) even though the width of the 511-keV peak was free to vary in the fit. The first peak has a β -detection efficiency consistent with ^{74}Ga β decay, while the later has a β -detection efficiency consistent with ^{74}Cu as well as a relative intensity in agreement with that given by Winger *et al.* (see Table II). Due to a lack of coincidence, the 516-keV γ ray could not be placed. The main hinderance is the overlap with the annihilation peak making it difficult to both fit the peak and obtain statistically significant coincidence results. Nevertheless, we are able to affirm the conclusion by Van Roosbroeck *et al.* that the 1164 keV and 2616 keV are not valid excitation states in ^{74}Zn .

B. Above 3.1 MeV

Above 3.1 MeV, Van Roosbroeck *et al.* proposed five energy levels which were not seen in the Winger *et al.* scheme. Our data was able to confirm all five of these levels, and add 27 new levels (see Figure 5). A notable characteristic of the Van Roosbroeck *et al.* scheme is the four levels above 4.5 MeV which are well separated from the main region below 3.0 MeV. These were the first hints for higher-lying states. One characteristic of many decay schemes with large decay windows is this grouping of levels within the scheme: discrete levels up to about 3 MeV, a 1–2-MeV range of sparsely-placed levels, and then a rather dense region around 5 MeV. Indeed, Figures 4 and 5 shows that this density of states exists in the ^{74}Zn level scheme. The density of states observed in this study in the lower region appears to increase up to 3165 keV. Though we have added several states just above this boundary, the density is clearly much lower and includes a 500-keV gap that leads up to the 4562-keV level. A second region of high density of states begins around this energy and continues up to about 5.2 MeV. After a 350-keV gap, another region of increased density of states is proposed. This middle-energy region is reminiscent of features of a “pygmy Gamov-Teller (GT)” region, or a group of excitation states which reflect the dipole resonant excitation from the lower-lying opposite-parity states. There is no clear reason to expect that the density of states above 4.5 MeV is complete; on the contrary, the unplaced γ rays listed in Table II indicates otherwise. Furthermore, the large Q_β window suggests that higher-lying states associated with the GT resonance may be expected to begin much closer to the Q_β limit.

C. γ -ray intensity normalization

Once the level scheme was constructed, coincidence summing corrections were made to all the observed rela-

tive γ -ray intensities associated with ^{74}Cu β decay. These are the intensities which are presented in Tables I and II. The relative intensities can be converted to absolute intensities by determining the intensity normalization factor for the reference 606-keV γ ray, i.e. the number of 606-keV γ rays emitted per 100 decays of ^{74}Cu . Direct β feeding to the ground state of ^{74}Zn involves a unique first-forbidden transition. Therefore, we will first assume very little, if any, direct feeding to the ground state as has been the case in the previous studies.[7, 8] Hence, the normalization factor for the 606-keV γ ray can be determined from the sum of the γ -ray relative intensity for all observed transitions to the ground state (115.8(10)), yielding 86.4(7)%. This value is in agreement with the NNDC value of 86.0(1.7) [16], primarily because all determinations of the value are based on the same four transitions to the ground state. However, many of the γ rays listed in Table II do not show $\gamma\gamma$ coincidences suggesting they could feed directly to the ground state. Furthermore, allowed β decays can directly feed 1^- states which can decay directly to the ground state by an E1 transition which might be stronger than the E1 transition to the 2_1^+ state. Therefore, to set a lower limit on the branching ratio, we assume that any γ rays in Table II with energies above 3 MeV which lack coincidence data or which cannot be logically placed elsewhere in the decay scheme will feed the ground state. The resulting total feeding to the ground state is 122.0(26)%. Consequently, we report the normalization factor based on the observed intensities as $86.4_{-6.1}^{+0.7}$. However, this value must be considered an upper limit for two reasons. First, there are still weak γ -ray transitions to the ground state which are not identified. Second, and more importantly, the assumption of no direct feeding to the ground state may not be valid. The 1418-, 1789-, and 2099-keV levels all show some apparent feeding from a first-forbidden unique β decay, so similar feeding to the ground state cannot be ignored. The importance of a direct measurement of the normalization factor for the 606-keV γ ray cannot be ignored.

D. Level feedings and $\log(ft)$ values

Using the summing corrected γ -ray intensities, estimated level feedings based on relative intensity were determined and are presented in Table III. Although these values are probably reasonable for the states above 3.0 MeV, the possibility of unplaced γ rays feeding into the lower-lying states could significantly change the total feeding. To test this possibility within the limitations of our data set, we made very speculative placements of the γ rays in Table II, as well as some unassigned γ rays, to determine the effect on the level feedings. All but two γ rays in Table II could be placed. Summing corrections were made based on the new level scheme and the β feedings determined. These values were used to modify the uncertainty limits on the feeding values listed

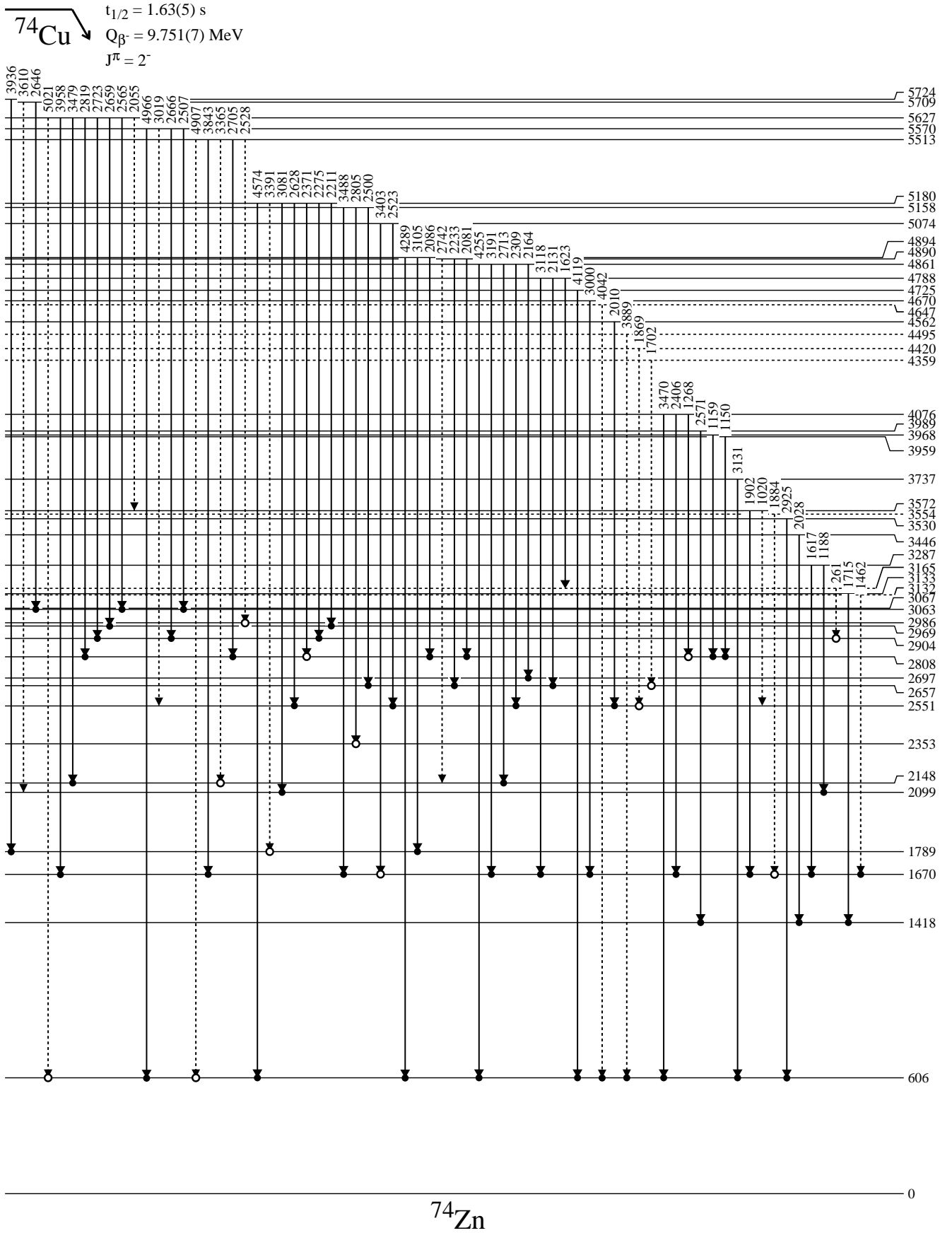


FIG. 5. Proposed decay scheme for ^{74}Cu determined in this analysis in the energy region above 3.1 MeV. See Section III-B for discussion. Solid dots indicate definite coincidences, while open dots indicate possible coincidences based on the statistical tests mentioned in the text.

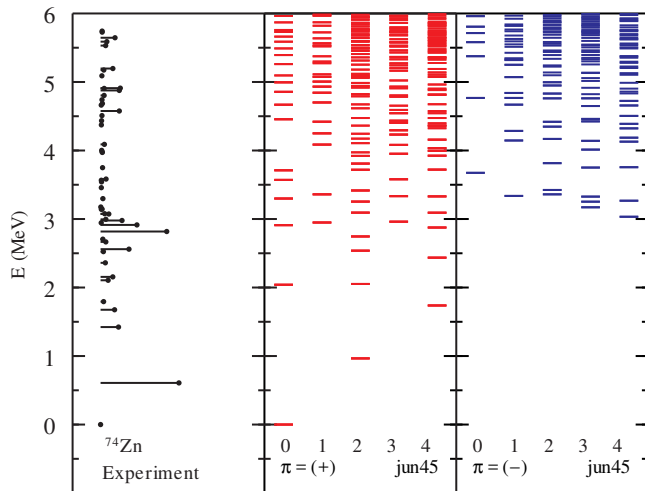


FIG. 6. Comparison of both positive and negative parity states predicted by the shell model for ^{74}Zn with the experimental level energies reported in this work.

in Table III. Additional feeding into a level results in an increase in the lower limit while additional feeding out of a level gives an increase in the upper limit. Additional feeding out of a level can result from changes in the summing correction.

The observed relative feedings can be converted to assumed absolute feedings using the normalization factor determined in the previous section. Although $\log(ft)$ values provide no definitive information on spin and parity, they can be used to as guides to distinguish between allowed and forbidden decays. Therefore, the $\log(ft)$ values listed in Table III were determined using the upper limit for the normalization factor (87.1) along with the maximum relative β feeding suggested by the data, and should only be considered lower limits to guide the discussion.

E. Shell Model Calculations

The level scheme in Figures 4 and 5 can be compared to shell model predictions using NUSHELLX [17]. We ran NUSHELLX using the jj44 model space, which assumes a doubly-magic ^{56}Ni core with two valence protons and sixteen valence neutrons. The interaction used in this space was the JUN45 [18], a Hamiltonian which is defined by four single-particle energies (SPE) and 133 two-body matrix elements (TBME). We ran the calculation with no restrictions over the spin range $0 \leq J \leq 4$ and with both parity options simultaneously for all states up to 6 MeV. We will not go into the specifics of the calculation since our interest is only to use the results to illuminate the experimental data. The comparison is shown in Figure 6. The experimental results are presented in the left panel with the widths scaled by the I_β values. The middle and

right panels show the positive and negative parity states, respectively, predicted by NUSHELLX. These results are discussed in the following section.

F. Spin and Parity Assignments

Of the new transitions added to the level scheme below 3.1 MeV, most have $I_\gamma \geq 0.35\%$. Since more than thirty γ rays placed in our scheme have lower intensities, we have a reasonable expectation that the level scheme populated by β decay below 3.1 MeV is nearly complete. Because of this, we can begin to propose spin and parity assignments to many of the levels above the first two excited states for the first time.

In the time since the Van Roosbroeck *et al.* paper, the ground state spin of ^{74}Cu has been measured to be $J^\pi = 2^-$ [19]. Van Roosbroeck *et al.* proposed spin 2 or 3 with a suggestion of negative parity based on $\log(ft) > 6.0$ for the 606-keV first excited 2^+ state, in agreement with the now-measured value. Our work shows little difference with $\log(ft) > 6.18$ (Table III).

The 606-keV first excited state has a spin/parity of 2^+ as shown in Coulomb excitation [20] and level lifetime [21] measurements in agreement with the expectations of systematics [7, 8]. The 1418-keV second excited state was also observed as an yrast excitation in the level lifetime measurement and assigned as a 4^+ state which confirms earlier speculation [7, 8]. Direct feeding to these first two states from higher lying states as well as transitions to the 0^+ ground state can limit the possible spin/parity assignments for those states. In addition, $E(4^+)/E(2^+) = 2.34$ is consistent with an anharmonic oscillator with moderate deformation suggesting a possible sequence of states, specifically expected 0^+ and 2^+ states at close to the same excitation energy. This pattern is also evident in the shell model calculations shown in Figure 6. With $\log(ft) > 6.64$ and $\log(f_{1u}t) > 8.86$ the transition is consistent with a unique first-forbidden decay, albeit at the lower limit for this transition type suggesting additional feeding intensity is missing.

The 1670-keV level was proposed as a 2^+ state by Winger *et al.* based on transitions to the ground and first excited states as part of the two-phonon excitation. Van Roosbroeck *et al.* reasoned that a possible 1^+ or 2^+ assignment was a better option due to systematics. Our results shed additional light on this assignment. Consider Figure 7, which shows the β feeding from the three β -decay measurements of ^{74}Cu . In the first two experiments, the 1670-keV level had a relative $I_\beta = 9.0$ and 7.0 , respectively, and $\log(ft)$ values of 5.5 and 6.4 , respectively [7, 8]. Our data has $I_\beta = 3.52_{-0.21}^{+0.38}$, a significant reduction from the previous experiments. This is due to the significant increase in the number of transitions identified as feeding the 1670-keV level. We calculated $\log(ft) > 6.66$, a notable increase over the two earlier measurements. What originally looked like an allowed transition from an expected 3^+ ^{74}Cu ground state to a

TABLE III. Information on the proposed levels in ^{74}Zn fed by ^{74}Cu , including the observed relative β -decay feeding, estimated lower limits on the $\log(ft)$ values, and proposed spin and parity assignments. See text for details.

Energy (keV)	I_β (rel)	$\log(ft)$	J^π	Energy (keV)	I_β (rel)	$\log(ft)$	J^π
605.766(11)	$19.7^{+1.1}_{-4.8}$	6.18	2^{+ab}	3571.57(7)	$1.38^{+0.19}_{-0.09}$	6.51	
1418.228(16)	$4.51^{+0.20}_{-1.21}$	6.64	4^{+ab}	3737.13(22)	0.50(5)	6.92	
1669.970(15)	$3.52^{+0.38}_{-0.21}$	6.66	$(2^+)^a$	3958.79(12)	0.44(4)	6.90	
1788.52(11)	$0.76^{+0.23}_{-0.41}$	7.22	(0^+)	3967.6(3)	0.39(7)	6.92	
2098.909(17)	$1.90^{+0.16}_{-0.29}$	6.80	(4^+)	3988.95(24)	0.28(3)	7.08	
2148.31(4)	3.07(11)	6.62	(2^+)	4076.14(16)	0.96(8)	6.52	
2352.94(3)	$1.20^{+0.19}_{-0.39}$	6.93	$(2^+, 3^+, 4^+)$	4359.1(4)	0.20(4)	7.06	
2515.65(12)	$0.71^{+0.05}_{-0.20}$	7.14	$(2^+, 3^+, 4^+)$	4420.2(4)	0.25(5)	6.94	
2551.479(19)	$7.14^{+0.21}_{-0.64}$	6.15	$(2^+, 3^+)$	4494.7(4)	0.35(4)	6.80	
2657.16(3)	$1.32^{+0.12}_{-0.19}$	6.83	$(2^+, 3^+, 4^+)$	4561.60(5)	$4.71^{+0.39}_{-0.07}$	5.66	$(1^-, 2^-, 3^-)$
2696.96(5)	$0.57^{+0.13}_{-0.30}$	7.13	$(1^+)^a$	4647.4(8)	0.17(11)	6.89	
2808.393(19)	$16.63^{+0.19}_{-0.90}$	5.72	(3^-)	4669.75(20)	$0.46^{+0.46}_{-0.04}$	6.36	
2904.32(3)	$9.14^{+0.14}_{-0.26}$	5.94	(3^-)	4724.8(4)	$0.36^{+0.04}_{-0.14}$	6.70	
2934.6(4)	0.16(4)	7.60		4787.89(13)	$1.21^{+0.08}_{-0.17}$	6.17	
2968.66(4)	$5.39^{+0.09}_{-0.35}$	6.16		4860.78(7)	$4.71^{+0.50}_{-0.10}$	5.53	$(1^-, 2^-, 3^-)$
2985.53(6)	$1.33^{+0.06}_{-0.17}$	6.75		4889.98(18)	0.91(10)	6.23	
3063.05(5)	$2.07^{+0.13}_{-0.08}$	6.53		4894.34(6)	$4.96^{+0.14}_{-0.19}$	5.52	$(1^-, 2^-, 3^-)$
3067.27(15)	1.04(9)	6.81		5073.6(4)	0.33(5)	6.58	
3131.5(4)	0.19(4)	7.49		5157.54(22)	0.81(9)	6.17	
3133.45(18)	0.39(4)	7.21		5179.51(9)	$3.09^{+0.13}_{-0.24}$	5.60	$(1^-, 2^-, 3^-)$
3164.90(13)	0.06(5)	7.80		5513.14(16)	1.28(8)	5.83	$(1^-, 2^-, 3^-)$
3286.82(15)	0.59(6)	6.86		5570.45(14)	$1.58^{+0.14}_{-0.08}$	5.74	$(1^-, 2^-, 3^-)$
3446.1(5)	0.19(5)	7.37		5627.26(8)	3.63(13)	5.34	$(1^-, 2^-, 3^-)$
3530.4(3)	0.24(3)	7.29		5709.0(3)	0.40(8)	6.17	
3554.1(4)	$0.19^{+0.11}_{-0.05}$	7.24		5724.1(4)	0.39(4)	6.24	

^a Previously proposed.

^b Confirmed by experiment [20, 21].

possible 2_2^+ [7] is now very strongly evident to be a first-forbidden transition from a 2^- ground state to the likely 2_2^+ state. Again, 1_1^+ cannot be ruled out, but systematics of the 2_2^+ along with the shell model calculations strongly support that this state should be assigned 2^+ .

Another interesting detail of the 1670-keV state is that the 1064-keV γ ray de-exciting this state has a higher I_γ than does the 1670-keV γ ray. This indicates that the state has a higher overlap with the 2_1^+ state than it does with the 0_1^+ state. This characteristic is seen in vibrational states, suggesting that the 1670-keV state shows some vibrational behavior.

The positive parity states shown in Figure 6 (middle panel) so far seem to match with the low-lying experimental states, apart from a scaling factor. The 1789-keV level only has one γ ray placed decaying out of it to the 2_1^+ state, making identification of this level's J^π difficult. We can recommend it as a positive-parity state due to its high $\log(ft) > 7.22$ and the NUSHELLX calculations which show no negative parity states this low. The transition to the 2_1^+ state but not the 4_1^+ state limits the spin/parity assignment to 0^+ or 1^+ , while the expectations for a two-phonon vibrational state as well as the NUSHELLX calculation suggest a 0^+ state in this energy region. Therefore we propose this to be the 0_2^+ state. The $\log(f_{1u}t) > 9.41$ is consistent with a unique first-

forbidden transition.

The 2099-keV level has a $\log(ft) > 6.80$ which places it firmly as a positive parity state, and the fact that it transitions only to 2^+ and 4^+ states suggests a 2^+ , 3^+ , or 4^+ assignment. Theory predicts a 2^+ or 4^+ state, while the experimental data hints at either the 2^+ or 3^+ assignment owing to the significant I_γ dominance of the 1493-keV γ ray ($I_\gamma = 10.27(8)$) to the 606-keV state over the much weaker 681-keV ($I_\gamma = 1.08(4)$) or 429-keV ($I_\gamma = 0.95(4)$) γ rays. The $\log(ft) > 6.62$ for the 2148-keV level, suggests this state is also a positive parity state. The transitions out of the 2148-keV level are only observed to go to the ground and the first excited states, limiting the assignment to 1^+ and 2^+ . The theory results indicate close-lying 2^+ and 4^+ states and no 3^+ states this low. We therefore propose 4_2^+ for the 2099-keV state and 2_3^+ for the 2148-keV state.

The 2353-, 2516-, 2551-, and 2657-keV levels are all very similar in that they decay to only 2^+ and 4^+ states and have a $\log(ft) > 6$ indicative of a first-forbidden decay to a positive parity state. Consequently, we tentatively propose a $J^\pi = 2^+$, 3^+ , or 4^+ assignment for these states. The 2353-keV level decays 68% of the time by the 935-keV γ ray to the 4_1^+ state suggesting it could include a significant component of a two-phonon excitation. However, there is no connection to the 2_2^+ state. A

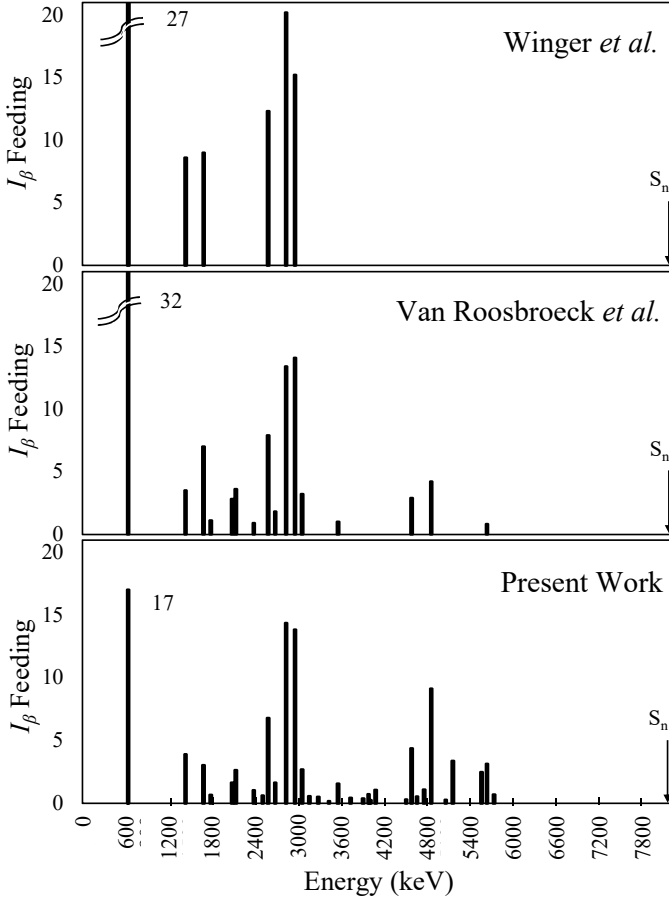


FIG. 7. Comparison of I_β profiles of each experiment. Bin widths were set to 200 keV.

very weak but unassigned 683-keV γ ray ($I_\gamma = 0.6(3)$) is observed but could not be definitively placed. The shell-model calculations suggest a slightly separated 2_4^+ state before the density of positive parity states increases rapidly. Hence, the 2353-keV level could be this state. The 2516-keV level decays equally to the 2_1^+ and 4_1^+ states, similar to the 2353-keV level. However, no further limitation on its J^π value is possible. The 2551-keV level shows strong transitions to the 2_1^+ and 2_2^+ states, with its most intense γ ray decaying to the 2099-keV (4_2^+) level. Its weakest transition, the 1133-keV γ ray, de-excites to the 4_1^+ state at 1418 keV. The state also shows stronger feeding ($\log(ft) > 6.15$ and $\log(f_{1ut}) > 8.26$) than others nearby, so this state appears to be fed by a non-unique first-forbidden transition allowing us to reject a possible 4^+ assignment. This state could be the expected lowest-lying 3^+ state, but further evidence is needed to make a firm assignment. The 2657-keV level decays primarily to the 2099- and 2353-keV levels suggesting a similar structure, but not providing information to further limit the J^π assignment.

The 2697-keV level shows a decay pattern distinctly different from the other states discussed so far with the exception of 2148-keV level. The two transitions which

de-exciting this level feed the 0_1^+ and 2_1^+ , while $\log(ft) > 7.13$ indicates a positive parity state. This suggests either $J^\pi = 1^+$ or 2^+ , in agreement with Van Roosbroeck *et al.* We looked for possible de-exciting transitions to other states but found none. If the 2697-keV state were 2^+ , we might expect to see more transitions to the 2^+ and 4^+ states. With the first four 2^+ states tentatively assigned, the NUSHELLX calculations indicate the first 1^+ state to occur at an energy lower than the 2_5^+ . Thus, we propose that the 2697-keV level is the first 1^+ state in the ^{74}Zn scheme. Above this energy, the density of positive-parity states precludes making any reasonable assignments.

The assumed β feeding, shown in Figure 7, has changed over the course of the three β decay studies. The profile has shifted higher as a reflection of the placement of higher states, resulting in a reduction of the intensities feeding to the lower states. What stands out in this figure is the pair of strongly-fed states at 2808 and 2904 keV. If these are negative parity states, then they will decay by E1 transitions to the lower-lying positive parity states. According to Figure 6, the first appearance of negative parity states is above 3 MeV, however, accounting for an assumed scaling factor reduces this energy to below 3 MeV. The 2808-keV level is the first reasonable candidate for a negative parity state, given the sudden increase in observed relative feeding and $\log(ft) > 5.72$ being lower than all lower lying states suggesting apparent strong feeding from the ^{74}Cu 2^- ground state. Although a first-forbidden transition is not ruled out, the lower $\log(ft)$ value makes it improbable. Transitions from the 2808-keV level de-excite to 2_1^+ , 2_2^+ , 4_2^+ , and possible 2_3^+ levels. Despite the NUSHELLX prediction of a 4^- state as the first negative parity state, a $\Delta J = 2$ β decay is ruled out, and such a state would not decay to the 2^+ states. The lowest-lying state showing decays to 4^+ states but not to 2^+ states is at 3133 keV. There is a triplet of 3^- states predicted by the NUSHELLX calculation. Shortly after the Van Roosbroeck *et al.* paper, the β decay of ^{72}Cu was measured [22], and a triplet of states at 2442, 2646, and 2909 keV were observed with spins of 3 or 4 proposed. If we use systematics, taking into account similar states in ^{70}Zn as well, we propose $J^\pi = 3^-$ for the 2808-keV level. The 2904-keV level is similar to the 2808-keV level. It has a reasonably large β feeding with $\log(ft) > 5.94$, and decays to the same basic set of lower-lying states. Therefore, we also propose this to be a 3^- state.

For the remainder of the level scheme it is difficult to make any firm assignments. As seen in Figure 6, the density of positive and negative parity states rises rapidly even if we limit the discussion to only those states feed by allowed or first forbidden decays. No states showing $\log(ft) < 5$ are observed because the allowed β strength has been split over a large number of states. We would expect to see a fall off in feeding by first-forbidden transitions as the negative parity states become available. However, $\log(ft) > 6$ values could be observed for either positive or negative parity states. Therefore, we

use $\log(ft) < 6$ values to postulate allowed β transitions for the 4562- (5.66), 4861- (5.53), 4894- (5.52), 5179- (5.60), 5513- (5.83), 5570- (5.71), and 5627-keV (5.34) levels, thus limiting their spins and parities to 1^- , 2^- , or 3^- .

It should be noted in Figure 7 that most of the levels' progressive changes in intensity can be easily attributed to our increasing knowledge of feeding to higher states. However, the 1418-keV level drops by about half from Winger *et al.* [7] to Van Roosbroeck *et al.* [8], then shows a small rise in our results. This is most easily explained as an artifact of the over-subtraction of the “off-resonance” spectrum by Van Roosbroeck *et al.*, where a very broad but relatively-low-count peak at around 806 keV in the off-resonance spectrum was enlarged in the subtraction process, leading to a smaller area for the 812-keV peak in their subtracted spectrum leading to a significant reduction in the expected I_β feeding to the 1418-keV level. In our work, $I_\beta = 4.51^{+0.20}_{-1.21}$ is in agreement with the value from Van Roosbroeck *et al.* only because of additional transitions identified as feeding the state. Including only those transitions identified by Van Roosbroeck *et al.* yields $I_\beta = 6.28(18)$.

IV. DISCUSSION

A. The pandemonium effect in ^{74}Zn

Since 1999 when it was first identified that incomplete β -decay schemes contributed to incorrect decay heat calculations, the pandemonium problem, efforts have been made to rectify this issue. In their first report, Yoshida *et al.* [3] provided a list of nuclides whose decay data discrepancy had the greatest influence on decay heat calculations. This list was comprised of a majority of the nuclei which have the highest yield in a fission reaction with reasonably large (> 3.0 MeV) Q_β windows. Recall that thermal fission events commonly result in two daughter nuclides whose masses lie within the $80 \leq A \leq 110$ (lower-mass daughter) and $125 \leq A \leq 155$ (higher-mass daughter) regions. Figure 8 [16] shows the lower-mass yield region for the two principal fission fuels, ^{235}U (top left) and ^{239}Pu (top right), with the magic nuclides for $N = 50$ and $Z = 28$ outlined with dark rectangles, ^{74}Zn indicated with a single open black box, and ^{74}Cu is indicated with a solid black box. The high-yield nuclei at the center of the pandemonium problem all lie in or adjacent to the dark red region (yield probability $\sim 10^{-1} - 10^{-3}$), with a similar situation occurring in the higher-mass region.

As mentioned in the Introduction, the pandemonium problem occurs as a result of the pandemonium effect in which weak feeding to an essentially continuous distribution of states (see Figure 6) results in the daughter nuclide's decay scheme catalogued in the database being incomplete. This is often the consequence of experiments which use high-resolution detectors to measure individual

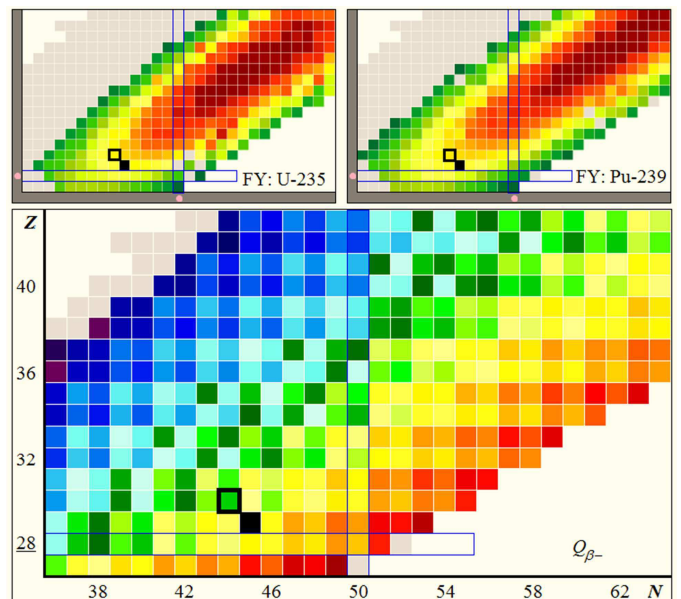


FIG. 8. (Color Online) Fission yields and Q_β windows in ^{74}Zn region centered near $N_{magic} = 50$, captured from the NNDC [16]. [Top] The lower-mass region of fission yield for both ^{235}U and ^{239}Pu , the principal fuels used in nuclear power plants. The dark red regions (yield probability $\sim 10^{-1} - 10^{-3}$) contain the nuclides from the Yoshida *et al.* [3] list of heaviest influence on the pandemonium problem. The orange and yellow regions have yield probabilities $\sim 10^{-4} - 10^{-8}$ and the green regions have $\sim 10^{-9} - 10^{-15}$. [Bottom] Q_β window for nuclides in the same region, where green represents $Q_\beta \sim 60 \text{ keV} - 3.6 \text{ MeV}$, yellow represents $Q_\beta \sim 5.3 - 10 \text{ MeV}$, and orange/red represents $Q_\beta > 10 \text{ MeV}$. The open black square indicates ^{74}Zn while the solid black square indicates ^{74}Cu .

γ -ray energies and intensities. Good coincidence data in these high-resolution experiments allows determination of the energy levels through coincidence reconstruction. As demonstrated here, decay schemes can be constructed from the ground state up but are limited by diminishing intensities of γ rays from high-lying states and suffers from the efficiency limitations of the detector. The use of a high-efficiency detector, on the other hand, has been successful at giving better information about β feeding to the high-energy region of the Q_β window. The basics of the difference between how high-resolution and high-efficiency detectors capture radiation and convert it to data signals can be reviewed in Reference [23], but the ultimate result is that the high-efficiency detector is able to capture *all* γ rays in a cascade. Capturing the sum of the γ rays severely limits its ability to resolve individual states, but it is able to give good information on direct feeding to the highest states in the decay scheme. In other words, the high-efficiency detector is utilized as a calorimeter for the decay due to strong coincidence summing. Because of this, use of these detectors is referred to as Total Absorption γ -ray Spectroscopy, or TAGS. The Yoshida *et al.* list, due to its high influence on the pandemonium problem, has been the primary fo-

cus of TAGS experiments in order to resolve the discrepancy [24]. However, this intense focus has the unintended consequence of being somewhat shortsighted in limiting the database which is designed to be used to accomplish the goal of correcting the β feeding functions used in decay heat calculations.

The high-energy region of nuclides with large Q_β windows remains a largely under-explored region of nuclear physics. The lower panel of Figure 8 displays the Q_β windows for nuclides in this region. Recent experiments have ventured beyond the pandemonium problem outlined in the Yoshida *et al.* list, employing TAGS measurements to help solve other problems. For example, Tain *et al.* performed a TAGS experiment on $^{87,88}\text{Br}$ and ^{94}Rb , known β -delayed neutron emitters, in order to demonstrate the emission of γ rays from states above the single-neutron separation energy, S_n [25]. Their results were not only used to contribute data for the decay heat database, but also were useful to r -process calculations which require good (n,γ) cross sections for nuclides far from stability. It should be noted that the $Q_\beta = 8975(4)$ for ^{88}Br and $Q_\beta = 10283(3)$ for ^{94}Rb [16]. Both are comparable with the Q_β window for ^{74}Cu ($Q_\beta = 9751(7)$).

Dombos, *et al.* [27] studied ^{76}Ga β decay, an isotone of ^{74}Zn , allowing systematics to be used in their comparisons. This TAGS experiment was geared toward the neutrino-less double- β decay in ^{76}Ge . They used the results from their TAGS data to extract the β -feeding intensities and Gamov-Teller transition strength distributions. As seen in Section III, the density of states in the 4.5-6 MeV region of the ^{74}Cu decay scheme shows signs of being a Gamov-Teller transition region. Indeed, many nuclei show such a profile: low-lying states showing an increasing density of states up to around 3 MeV, a gap of sparse states, a pygmy Gamov-Teller region in ~ 4 -7 MeV range, and, according to several TAGS measurements on large Q_β windows, a region of increasing density of states above the pygmy GT leading up to S_n or Q_β .

The pandemonium effect is becoming quite apparent in the results presented here. Table IV shows the progression of select absolute I_β values from Winger *et al.* to Van Roosbroeck *et al.* to this work. The changes are the result of correcting the placement of γ rays as well as the addition of new γ rays affecting the feeding into and out of each level. For example, the observed increase in feeding to the 606-keV level between Winger *et al.* and Van Roosbroeck *et al.* is due to correcting placement of the 558- and 2010-keV γ rays. The addition of γ rays can work to either decrease or increase the observed feeding to a level. Nevertheless, as can be seen, a notable shift in the feeding intensity to each excitation energy state occurs as the high-resolution detector setup and ^{74}Cu beam production techniques have improved. Specifically, possible direct feeding to the low-lying states is reduced as additional feeding transitions are established, while higher-lying states see increased intensity as additional de-exciting transitions are identified. However, the results are still incomplete. The maximum proposed en-

TABLE IV. Select absolute I_β values from each of the three measurements of ^{74}Cu . Below the main table the energy of the highest proposed state as a percentage of Q_β is given. See text for discussion.

E_{level} (keV)	Winger	Van Roosbroeck	Current Work
606	27	32	17.0
1418	8.6	3.5	3.9
1670	9.0	7.0	3.0
2552	12.3	7.9	6.2
2808	20.2	13.4	14.4
2904	9.1	8.5	7.9
4562	--	2.9	4.1
4894	--	2.2	4.3
5627	--	0.8	3.1
Index	30.4%	57.7%	58.7%

ergy level is still less than 60% of the available Q_β energy window. We also have a significant number of unplaced γ rays (see Table II). Even with the speculative placement of these γ rays mentioned earlier, the maximum energy is not increased above 5.8 MeV, and the additional energy levels provide an almost uniform background filling in the gaps in the proposed decay scheme above 3 MeV (see Figure 5). Extending the decay scheme to higher energies using a high-resolution system will require a significant increase in detector efficiency or beam intensity as our γ -ray singles spectrum goes to “zero” counts at about 5.3 MeV and the add-back spectrum only shows a smoothly falling continuum out to 6.5 MeV with no discernable structure. In addition, $\gamma\gamma$ coincidence data is needed to establish the level scheme. What becomes very apparent in the coincidence data is that unresolved doublets are a significant issue. Hence, properly assigning intensity to a particular transition, and therefore energy level, can require major effort for minimal information. Consequently, learning more about excited states in ^{74}Zn above 5.8 MeV will require a TAGS measurement.

V. TAGS FOR ^{74}Cu

To further determine the impact that a TAGS measurement for ^{74}Cu would have, a simulated TAGS spectrum for each of the three measurements for this nuclide has been produced and can be seen in Figure 9. In this figure, the response of the Modular Total Absorption Spectrometer (MTAS) [28] is simulated as if each of the three high-resolution measurements performed on ^{74}Cu were a full account of the β -decay spectrum from that isotope. The first measurement, by Winger *et al.* (black trace), is largely unremarkable, having no sign of structure above 3 MeV. However, when the second experiment (Van Roosbroeck *et al.*, in cyan) is shown in comparison, the profile displays a notable shift to higher

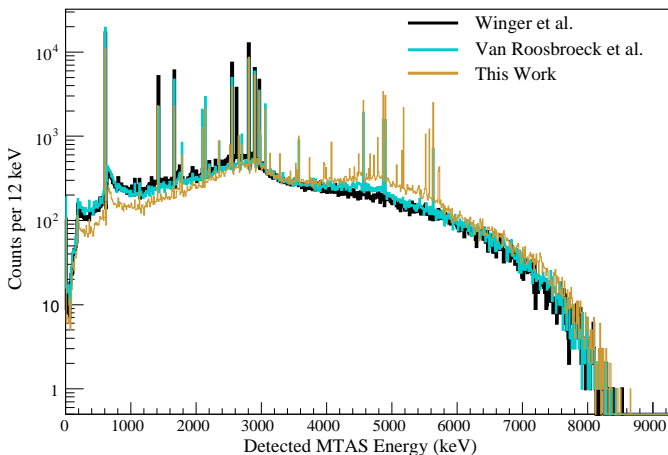


FIG. 9. (Color Online) A Modular Total Absorption Spectrometer (MTAS) simulated response for each of the three decay schemes performed to date. The black trace is based on the scheme from Winger *et al.*, the cyan trace is from the work by Van Roosbroeck *et al.*, and the brown trace reflects the experiment reported here. See text for discussion.

energies. The importance of having good information on even middle-lying levels (4-6 MeV) cannot be ignored. Finally, the response predicted by the current work is shown by the brown trace. The 606 keV energy level background profile for the current work is one third that of the Winger *et al.* simulation. There is relative stability among the states which exist between 2 and 3 MeV, which may give insight to the particular J^π of these levels. In the 4-6 MeV range, the feeding characteristics to these levels is quite prominent. If we accept the standards put forth by Algora *et al.* [5], we can use the ratio of the maximum energy level known to be fed by β decay to the total Q_β energy to indicate progress made in each successive measurement of the ^{74}Cu β decay. This value is indicated by Index in Table IV. The simple shifting of the overall profile by doubling the maximum observed energy level has led to an unmistakable buildup of MTAS response going into the highest accessible energies projected for these simulations. As shown in Table IV, direct β feeding to levels below 3 MeV has shown a drop over the three experiments while feeding to levels above 3 MeV has increased. The maximum energy level nearly doubled between the Winger *et al.* and the Van Roosbroeck *et al.*. However, despite having added 79 γ rays and 29 energy levels, we have only slightly increased the maximum energy level which is still well below the arbitrary threshold of 70% for the pandemonium problem as suggested by Algora *et al.* [5] as a convenient means for comparison between decays. Although the current results do not push up the maximum energy, Figure 9 shows a significant increase in the total energy spectrum for the 4-6 MeV range. One can only imagine at this stage how the profile of the 6-9-MeV range will look when an actual TAGS measurement is performed on this nuclide.

As mentioned previously, the data collected in this

experiment has also yielded new information about the β decay of ^{74}Ga . One preliminary detail is that the β -feeding directly to the first excited state (596 keV) in the ^{74}Ge daughter has been reduced from the previously-published value of $I_\beta = 4.7\%$ to approximately zero. Systematics of the $A = 74$ isobars suggest that the first excited level of ^{74}Zn and ^{74}Ge should have similar structure. ^{74}Ge is a stable isotope, and its level scheme has been well-documented. The ground state of ^{74}Ga was recently measured and tentatively assigned to be $J^\pi = 3^-$ [29]. Consequently, the β decays of ^{74}Cu and ^{74}Ga to the 2_1^+ state in the daughter will be first forbidden. While $\log(ft) = 6.2$ seems to fit this transition, it is on the lower limit of the expected range. Hence, in comparison to ^{74}Ga , it is reasonable to expect that the feeding to the 606 keV state is still being overestimated. This issue can easily be resolved with a TAGS study of the β decay of ^{74}Cu .

In short, although ^{74}Cu is not considered a major contributor to decay heat, it is one of many ideal candidate nuclides with an attractive Q_β window, relatively high S_n , and spin-parity characteristics compared to its daughter that increase the likelihood of feeding to high-lying γ -emitting states. By broadening the TAGS database with good I_β functions for these peripheral thermal-fission products, the decay heat community will have a much more comprehensive resource from which to develop superior models for compensating for the pandemonium effect in unmeasured nuclides relevant to decay heat.

VI. CONCLUSION

The β decay of ^{74}Cu has been updated based on the analysis presented in this paper. By using a high-precision mass separator, it was possible to achieve a reasonably pure beam of ^{74}Cu which had not been previously accomplished. This prevented the copper γ -ray peaks from being obscured by γ -ray peaks from the zinc and gallium isotopes in the decay chain, and improved statistics were obtained over previous measurements.

A total of 170 γ rays were assigned to ^{74}Cu β decay, of which 111 were successfully placed in a 50-level decay scheme, itself consisting of 29 new levels. Feeding intensities and $\log(ft)$ values were determined, and compared against previous results. A simulation of the response of a TAGS spectrometer assuming each measurement of ^{74}Cu gave a complete scheme further demonstrated that β -feeding to higher-lying states was not only reasonable, but very likely. This led to a conclusion that a Total Absorption γ -ray Spectroscopy (TAGS) measurement of this nuclide is necessary in order to provide an accurate β function for decay heat calculations.

VII. ACKNOWLEDGMENT

This work was performed under the support of the U.S. Department of Energy under contracts DE-FG02-96ER41006 and DE-SC00144448. Additional sup-

port was provided by Polish National Science Center under Contract No. UMO-2015/18/E/ST2/00217, and by the Office of Nuclear Physics, U. S. Department of Energy under contracts no. DE-AC05-00OR22725 (ORNL), DE-FG02-96ER40983 (UTK), DE-AC05-06OR23100 (ORAU), and DE-AC02-05CH11231 (UC)

-
- [1] K. Way, E. P. Wigner, *Phys. Rev.* **73** 1318 (1948).
 - [2] J. Griffin, *Phys. Rev.* **134**, B817 (1964).
 - [3] T. Yoshida *et al.*, *J. Nuc. Sci. Technol.* 36, No. 2 135 (1999).
 - [4] J. C. Hardy *et al.*, *Phys. Lett.*, Vol. 71 B, No. 2, 307 (1977)
 - [5] A. Algora *et al.*, *J. Korean Phys. Soc.* 59, No. 2, 1479 (2011).
 - [6] W. J. Huang *et al.*, *Chin. Phys.* C41030003 (2017).
 - [7] J. A. Winger *et al.*, *Phys. Rev. C* **39** vol 5 1976 (1989).
 - [8] J. Van Roosbroeck *et al.*, *Phys. Rev. C* **71** 054307 (2005).
 - [9] T. Yoshida *et al.*, *J. Korean Phys. Soc.* 59, No. 2, 1543 (2011).
 - [10] 2008APS..SES.EA004I S. V. Ilyushkin *et al.*, APS South-eastern Section Meeting Abstracts, (2008).
 - [11] S. V. Ilyushkin *et al.*, *Phys. Rev. C* **83**, 014322 (2011).
 - [12] M. Lipoglavšek *et al.*, *Nucl. Instrum. Meth. A***557**, 523 (2006).
 - [13] M. A. Schumaker *et al.*, *Nucl. Instr. and Meth A***570**, 437 (2007).
 - [14] U. Rizwan *et al.*, *Nucl. Instrum. Meth. A***820**, 126 (2016).
 - [15] S. V. Ilyushkin *et al.*, *Phys. Rev. C* **80**, 054304 (2009).
 - [16] Natl. Nucl. Database Ctr., *www.nndc.bnl.gov* (2016).
 - [17] B. A Brown, W. D. M. Rae, *Nucl. Data Sheets* **120**, 115 (2014).
 - [18] M. Honma *et al.*, *Phys. Rev. C* **80**, 064323 (2009).
 - [19] K. T. Flanagan *et al.*, *Phys. Rev. C* **82**, 041302(R) (2010).
 - [20] J. Van de Walle *et al.*, *Phys. Rev. C* **79** 014309 (2009).
 - [21] C. Louchart *et al.*, *Phys. Rev. C* **87** 054302 (2013).
 - [22] J.-C. Thomas *et al.*, *Phys. Rev. C* **74** 054309 (2006).
 - [23] G. F. Knoll, *Radiation Detection and Measurement*, 3rd ed. (Wiley, New York, 2000) 114-116.
 - [24] P. Dimitriou and A. L. Nichols, IAEA Report No. INDS(NDS)-0676, <http://www-nds.iaea.org/publications>(2015).
 - [25] J. L. Tain, E. Valencia, A. Algora, *et al.*, *Phys. Rev. Lett.* **115**, 062502 (2015).
 - [26] B. C. Rasco *et al.*, *Phys. Rev. Lett.* **117**, 092501 (2016).
 - [27] A. C. Dombos, D.-L. Fang, A. Spyrou, *et al.*, *Phys. Rev. C* **93**, 064317 (2016).
 - [28] M. Wolinska-Cichocka *et al.*, *Nucl. Data Sheets* **120**, 22 (2014).
 - [29] E. Mané, *et al.*, *Phys. Rev. C* **84**, 024303 (2011).